Journal of
Synchrotron Radiation

ISSN 0909-0495

Received 5 April 2005
Accepted 29 June 2005

X-ray emission spectroscopy with a laser-heated diamond anvil cell: a new experimental probe of the spin state of iron in the Earth's interior

Jung-Fu Lin,[a]*‡ Viktor V. Struzhkin,[a] Steven D. Jacobsen,[a] Guoyin Shen,[b] Vitali B. Prakapenka,[b] Ho-Kwang Mao[a] and Russell J. Hemley[a]

[a]Geophysical Laboratory, Carnegie Institution of Washington, 5251 Broad Branch Road NW, Washington, DC 20015, USA, and [b]Consortium for Advanced Radiation Sources, The University of Chicago, Chicago, IL 60637, USA. E-mail: j.lin@gl.ciw.edu

Synchrotron-based X-ray emission spectroscopy (XES) is well suited to probing the local electronic structure of 3*d* transition metals such as Fe and Mn in their host phases. The laser-heated diamond anvil cell technique is uniquely capable of generating ultra-high static pressures and temperatures in excess of 100 GPa and 3000 K. Here X-ray emission spectroscopy and X-ray diffraction have been interfaced with the laser-heated diamond cell for studying the electronic spin states of iron in magnesiowüstite-$(Mg_{0.75},Fe_{0.25})O$ and its crystal structure under lower-mantle conditions. X-ray emission spectra of the ferrous iron in a single crystal of magnesiowüstite-$(Mg_{0.75},Fe_{0.25})O$ indicate that a high-spin to low-spin transition of ferrous iron occurs at 54 to 67 GPa and 300 K and the ferrous iron remains in the high-spin state up to 47 GPa and 1300 K. This pilot study points to the unique capability of the synchrotron-based XES and X-ray diffraction techniques for addressing the issue of electronic spin transition or crossover in 3*d* transition metals and compounds under extreme high-*P*–*T* conditions.

© 2005 International Union of Crystallography
Printed in Great Britain – all rights reserved

Keywords: X-ray emission spectroscopy; laser-heated diamond cell; electronic spin state; magnesiowüstite; high pressure.

1. Introduction

X-ray emission spectroscopy (XES) using a highly intense synchrotron X-ray source is well suited to probing the existence of the local high-spin or low-spin state in transition metals and transition metal compounds under high pressures in a diamond anvil cell (DAC). Synchrotron-based XES has been used to study pressure-induced high-spin to low-spin transitions in iron- and manganese-containing systems such as wüstite (FeO) (Badro *et al.*, 2002), troilite (FeS) (Rueff, Kao *et al.*, 1999), hematite (Fe_2O_3) (Badro *et al.*, 1999), magnesiowüstite [(Mg,Fe)O] (Badro *et al.*, 2003; Lin, Struzhkin *et al.*, 2005), ferromagnesian silicate perovskite [$(Mg,Fe)SiO_3$] (Badro *et al.*, 2004; Li *et al.*, 2004), iron alloys (Lin, Struzhkin *et al.*, 2004; Rueff *et al.*, 2001, 2002) and manganese oxide (MnO) (Yoo *et al.*, 2005), providing a deeper understanding of magnetic and electronic properties of important planetary materials at high pressures. In this technique, the electronic spin state of ferrous iron is characterized by the appearance of the satellite emission peak (K'_β) located in the lower energy region of the main emission peak ($K_{\beta 1,3}$) of ~7058 eV, which is a result of the 3*p*–3*d* core–hole exchange interaction in the final state of the emission process. On the other hand, the collapse of the magnetization of ferrous Fe is characterized by the disappearance of the low-energy satellite owing to the loss of the 3*d* magnetic moment (Peng *et al.*, 1994; Hölzer *et al.*, 1997; Rueff, Krisch *et al.*, 1999; Rueff *et al.*, 2001; Wang *et al.*, 1997).

Previous theoretical and experimental studies on the electronic spin transitions of 3*d* metals in their host phases have provided new insight into the effects of pressure on electronic structure (Sherman, 1988, 1991; Cohen *et al.*, 1997; Milner *et al.*, 2004), but the effects of temperature on the spin state of transition metals at high pressures have been restricted to theoretical and thermodynamic calculations (Badro *et al.*, 2003, 2004; Lin, Struzhkin *et al.*, 2005; Sturhahn *et al.*, 2005). Based on thermodynamic considerations, the effect of temperature on the high-spin to low-spin transition in iron is calculated by integrating the Clapeyron equation under high temperatures, where entropy and volume changes are estimated (Badro *et al.*, 2004; Li *et al.*, 2004; Lin, Struzhkin *et al.*, 2005). At the spin transition, the free energy change (ΔG) is the sum of the electronic internal energy change (ΔU), entropy change ($T\Delta S$) and volume change ($P\Delta V$) between

‡ Now at Lawrence Livermore National Laboratory, Livermore, CA 94551, USA.

the high-spin and low-spin configurations at a certain temperature (T) (Sherman, 1988; 1991), *i.e.* $\Delta G = \Delta U - T\Delta S + P\Delta V$.

It has been argued that the electronic transition is most of the time a density-driven transition that occurs at a given critical density, independently of pressure or temperature (Badro *et al.*, 2004). However, recent calculations using crystal field theory and an extended Bragg–Williams mean-field theory to model the temperature effects on the electronic high-spin to low-spin transition of iron in the host minerals and on the iron–iron interactions on the 3*d* energy levels of the iron show that the behavior of the mineral can be complex if the energy difference between high-spin and low-spin states is comparable with the thermal energy k_BT (with temperature T and Boltzmann's constant k_B), indicating that the spin transition of iron in the mantle host phases should occur over an extended pressure–temperature range (Sturhahn *et al.*, 2005). Although an isostructural first-order Mott transition in MnO has been observed at 105 GPa and 300 K, based on high-resolution XES and X-ray diffraction data, it is suggested that such a transition should end at a critical temperature point and a smooth spin crossover should occur above the critical point (Yoo *et al.*, 2005). On the other hand, the volume change associated with the high-pressure isosymmetric electronic transition in f.c.c. Ce (I) to Ce (IV), a rare earth lanthanide, is 13% at room temperature. The volume change gradually vanishes with increasing temperature along the phase transition boundary, and the electronic transition becomes undetectable in terms of volume change at approximately 2.2 GPa and 613 K (Gschneidner *et al.*, 1962; Davis & Adams, 1964), indicating a critical point of the transition at high pressure and temperature. The electronic spin transition of iron in magnesiowüstite also occurs as an isosymmetric transition in the B1 structure with a volume change of 1.6% for $(Mg_{0.4},Fe_{0.6})O$ at around 95 GPa and a significant effect on the incompressibility across the transition for $(Mg_{0.83},Fe_{0.17})O$ (Lin, Struzhkin *et al.*, 2005). It is thus necessary to study the temperature effects on the electronic spin transition of iron in the mantle host phases before applying the results to understand the geophysics and geochemistry of the Earth's interior.

The externally heated diamond anvil cell (EHDAC) technique has been commonly used to study material properties under high pressures and temperatures, but the use of a Be gasket in the XES study limits the application of the EHDAC technique because a Be gasket easily loses its strength to hold the sample at high temperatures. On the other hand, the laser-heated diamond anvil cell (LHDAC) technique has become the premier method for generating ultra-high static pressures and temperatures in excess of 100 GPa and 3000 K, corresponding to the conditions at the core–mantle boundary of the Earth's interior. Recently, the LHDAC technique has also been used in conjunction with *in situ* X-ray diffraction, nuclear resonant inelastic X-ray scattering, synchrotron Mössbauer spectroscopy and *in situ* Raman spectroscopy to study crystal structures and properties of materials under extreme conditions (Shen *et al.*, 2001; Lin, Santoro *et al.*, 2004; Lin, Sturhahn *et al.*, 2004, 2005; Santoro *et al.*, 2004; Zhao *et al.*, 2005). These studies have yielded data on the phase diagram, equation of state (EOS), elasticity and phonon density of states (DOS) of planetary materials. Owing to recent design improvements in LHDAC systems, it is now technically feasible to continuously laser-heat a sample in a diamond cell for up to 12 h (Lin, Stuhrhahn *et al.*, 2004), suitable for other methods such as XES which require lengthy data-collection times.

Direct measurements of the XES spectra under high pressures and temperatures would thus provide a critical test of theoretical and thermodynamic predictions on the electronic transitions of iron in oxides and silicates relevant to the Earth's interior. Here we describe the application of the LHDAC technique to XES studies using a single crystal of magnesiowüstite-$(Mg_{0.75},Fe_{0.25})O$ as an example. *In situ* XES and X-ray diffraction spectra of the sample were obtained up to 47 GPa and 1300 K. X-ray emission spectra reveal that a high-spin to low-spin transition of ferrous iron in $(Mg_{0.75},Fe_{0.25})O$ occurs at 54 to 67 GPa and 300 K and that the sample remains in the high-spin state up to 47 GPa and 1300 K (1200 km-depth in the Earth), whereas the X-ray diffraction patterns are used to confirm the B1 crystal structure of the laser-heated sample. Future improvements in the techniques are also discussed in this paper.

2. System set-up and sample configuration

A Rowland circle spectrometer of diameter 1 m in the vertical scattering geometry was configured around the double-sided laser-heating system at the GSECARS sector of the Advanced Photon Source (APS), Argonne National Laboratory (ANL) for X-ray emission studies of iron in magnesiowüstite under high pressures and high temperatures (Figs. 1–3). The use of the vertical geometry minimizes the X-ray emission background from Fe impurities in the Be gasket material, and minimizes the effects of pressure gradients for large samples. A Si(333) single-crystal wafer glued onto a spherical substrate of diameter 1 m was used as the analyzer, and a Peltier-cooled silicon detector with 5 mm^2 detection area and 500 μm in thickness (AMPTEK XR_100CR) was used to detect the emitted X-ray fluorescence. The Rowland circle spectrometer was shielded by the flight tubes which were filled with helium gas to reduce absorption by air.

Beveled diamonds with an inner culet of 150 μm and outer culet of 300 μm were used to pre-indent a beryllium gasket to a thickness of 25 μm. A hole of diameter 250 μm was drilled into the indented area and filled with amorphous boron as an inner insert gasket. The boron gasket insert was pre-indented to 25 μm and a 100 μm hole was drilled into it as the sample chamber. The use of the amorphous boron insert increases the thickness of the sample chamber (Lin *et al.*, 2003), making XES at higher pressure with a LHDAC possible. We prepared a sandwich sample configuration with a single-crystal sample of thickness 12 μm and diameter 70 μm in the middle and dried NaCl, for the thermal insulator and pressure medium, on both sides of the sample (Fig. 2). A Nd:YLF laser, operating in continuous donut mode (TEM_{01}), was used to heat the sample from both sides of the DAC (Shen *et al.*, 2001) (Fig. 3). During

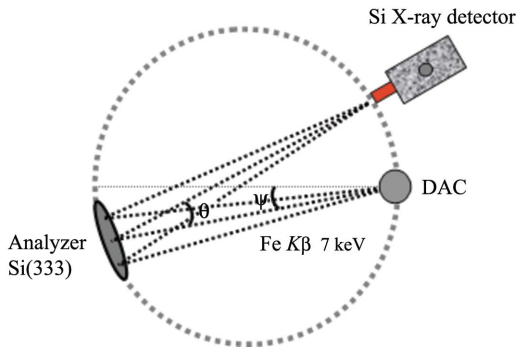

Figure 1
Schematic of the Rowland circle spectrometer of diameter 1 m in the vertical scattering geometry. A Si(333) single-crystal wafer glued onto a spherical substrate was used as the analyzer, and a Peltier-cooled silicon detector (AMPTEK XR_100CR) was used to detect the emitted X-ray fluorescence. The Fe K_β emission spectra were collected through a Be gasket which is transparent to the X-ray energy range of approximately 7 keV.

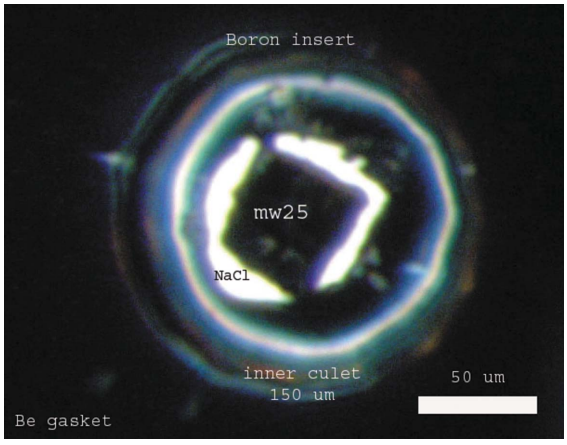

Figure 2
Photograph of a single crystal of magnesiowüstite-[$(Mg_{0.75},Fe_{0.25})O$] in the ⟨110⟩ orientation at 47 GPa and 300 K (central dark part of the picture). Both transmitted and reflected light source were used. Beveled diamonds with an inner culet of 150 µm and outer culet of 300 µm were used. Amorphous boron was used as an inner insert gasket and beryllium was used as an outer gasket to confine the amorphous boron. The sample chamber was originally about 100 µm in diameter. Use of the amorphous boron insert increases the thickness of the sample chamber (Lin *et al.*, 2003), making X-ray emission spectroscopy with a laser-heated diamond anvil cell possible. A sandwich configuration comprising the sample and dried NaCl as the thermal insulator and pressure medium on both sides of the sample was used. Pressure was determined from the ruby fluorescence shift, EOS of NaCl or EOS of the sample.

the experiments, the diameter of the laser beam at the sample position was about 25 µm. Greybody temperatures were determined by fitting the thermal radiation spectrum between 670 nm and 830 nm to the Planck radiation function.

A monochromatic X-ray beam of 14 keV was focused down to approximately 7 µm vertically and horizontally at the sample position, insuring that the X-ray fluorescence signals were only collected from the laser-heated area. The Fe K_β emission spectra were collected by the silicon detector through a Be gasket and a Si(333) analyzer in the Rowland circle geometry. The counting time for each XES spectrum was about 30 min and typically eight spectra were collected at the

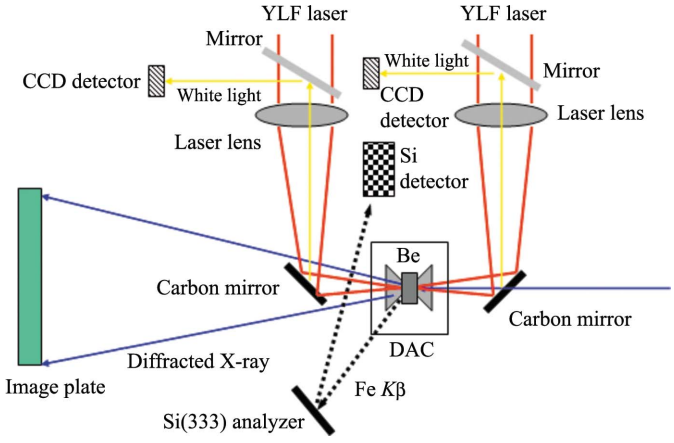

Figure 3
Schematic of the X-ray emission spectroscopy with laser-heated diamond anvil cell experiments. The YLF laser beam is focused to 25 µm onto both sides of the sample surfaces. The diameter of the focused X-ray beam at 14 keV was approximately 7 µm (FWHM); the small beam size ensured that the X-ray emission signal from the sample was only measured within the laser-heated spot of 25 µm. The single-crystal magnesiowüstite [$(Mg_{0.75},Fe_{0.25})O$] sample was loaded into the sample chamber of a diamond cell. The Fe K_β fluorescence lines were collected through the Be gasket by a 1 m Rowland circle spectrometer in the vertical scattering geometry. An image plate (MAR345) was used to collect diffracted X-rays in the forward direction.

same pressure and temperature and co-added. The energy of the monochromatic X-ray can be adjusted to allow the collection of X-ray diffraction patterns using monochromatic X-rays with a higher energy of approximately 35 keV. Since the single crystal of $(Mg_{0.75},Fe_{0.25})O$ was pre-oriented in the ⟨110⟩ orientation, sharp and symmetric zone-diffraction spots of the sample were collected using a MAR image plate simultaneously (Fig. 3) (see Jacobsen *et al.*, 2005). *In situ* X-ray diffraction was used to confirm the B1 structure and compositional homogeneity of the laser-heated sample during the high *P*–*T* XES measurements.

3. Results and discussion

X-ray emission spectra of iron in magnesiowüstite-$(Mg_{0.75},Fe_{0.25})O$ were collected up to 79 GPa at 300 K and 47 GPa at 1300 K (Figs. 4 and 5). The presence of the satellite peak (K'_β) at 47 GPa and 300 K is characteristic of the high-spin state of iron. XES studies of the Fe K_β fluorescence lines have revealed that a high-spin to low-spin transition occurs at 54 to 67 GPa and 300 K in $(Mg_{0.75},Fe_{0.25})O$ (Lin, Struzhkin *et al.*, 2005). On the other hand, the shape and intensity of the fluorescence lines remain similar at 47 GPa and 1300 K, indicating that iron in the sample is in the high-spin state as the pronounced K'_β peak is still observed (Fig. 5). Based on thermodynamic considerations of the volume and energy change across the transition (Burns, 1993), it is found that, for a magnesiowüstite containing ∼24% FeO, the Clapeyron slope of the high-spin to low-spin transition is shifted to ∼120 GPa at 2500 K (Lin, Struzhkin *et al.*, 2005). Our results indicate a positive Clapeyron slope of the high-spin to low-spin transition of ferrous iron in magnesiowüstite-

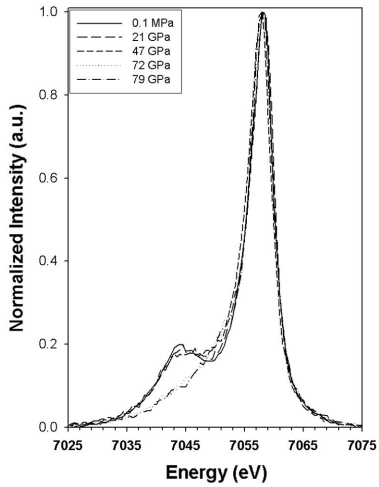

Figure 4
X-ray emission spectra of Fe K_β collected from a single crystal of magnesiowüstite-$(Mg_{0.75},Fe_{0.25})O$ at high pressures. The spectrum under ambient conditions was measured outside the DAC. The spectra were normalized to unity and shifted in energy to compensate for the pressure-induced shift of the line maximum based on the main fluorescence peak (K_β) at 7058 eV. The presence of the satellite peak (K'_β) at 0, 21, 47 GPa and 300 K is characteristic of the high-spin state of iron whereas the disappearance of the satellite peak at 72 and 79 GPa indicates the occurrence of the low-spin state of ferrous iron in $(Mg_{0.75},Fe_{0.25})O$ (Lin, Struzhkin *et al.*, 2005).

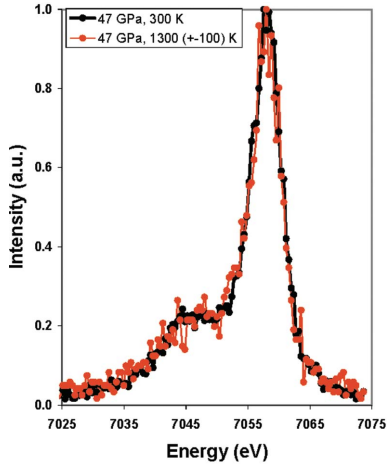

Figure 5
X-ray emission spectra of Fe K_β collected from a single crystal of magnesiowüstite-$(Mg_{0.75},Fe_{0.25})O$ in the ⟨110⟩ orientation in a laser-heated DAC. The sample remains in the high-spin state at 47 GPa and 1300 K as the pronounced K'_β peak is still observed. Lines through the data points are guides to the eyes. The error on the energy resolution is less than 1 eV whereas the error on the intensity is approximately 5% of the intensity.

$(Mg_{0.75},Fe_{0.25})O$, and application of the current techniques to higher pressures and temperatures would help reconcile the potential temperature-induced electronic spin crossover of iron in magnesiowüstite and ferromagnesian silicate perovskite in the Earth's lower mantle.

The electronic transition in magnesiowüstite and manganese oxide has been observed to cause a volume decrease and to affect the incompressibility and electrical conductivity of the sample (Shannon & Prewitt, 1969; Patterson *et al.*, 2004; Lin, Struzhkin *et al.*, 2005; Yoo *et al.*, 2005). Although the electronic spin transition of iron in magnesiowüstite is an isosymmetric transition at high pressures and room temperature (Lin, Struzhkin *et al.*, 2005), it has been suggested that the electronic transition would result in a phase separation between the iron-rich high-spin state and magnesium-rich low-spin state (Badro *et al.*, 2003) at high pressures and temperatures, causing two compositionally distinct phases. Therefore, it is crucial to simultaneously determine the crystal structure and to index the cell parameters of the sample while the XES spectrum is collected in a LHDAC. The determination of the cell parameters under high pressures and temperatures can also help understand the temperature effects on the volume change and elasticity change across the transition. Although the XES technique is only sensitive to the local magnetic moment of iron in the sample, the high-quality pre-oriented single-crystal sample of magnesiowüstite-$[(Mg_{0.75},Fe_{0.25})O]$ (Jacobsen *et al.*, 2002) provides high-resolution X-ray diffraction patterns, which are useful in identifying slight structural changes and potential compositional variation in the laser-heated sample. The integrity of the single-crystal sample is maintained at high pressures and temperatures as revealed by the sharp and symmetric diffraction spots. *In situ* X-ray diffraction patterns of the heated sample show that the sample remains in the B1 structure up to 47 GPa and 1300 K. The precision in cell parameters by full least-squares methods is typically less than a few parts in 10^4, which is approximately a factor of five better than that in power diffraction studies.

The pressure-induced electronic spin transitions in Fe-, Mn- and Co-containing materials have been well studied under high pressures and room temperature. The electronic transitions are either isosymmetric or concurrent with a structural phase transition. XES together with *in situ* X-ray diffraction in a LHDAC represents a new powerful technique for characterizing the electronic transition under extreme pressure–temperature conditions. It typically took at least 4 h to collect sufficiently accurate X-ray emission spectra in the current experimental settings at GSECARS, APS on $(Mg_{0.75},Fe_{0.25})O$. Optimization of the efficiency in the X-ray and laser optics (the flux of the incident X-ray source) and the Rowland circle spectrometer (analyzer and detector) will be beneficial for the measurements. With these future improvements, simultaneous XES and X-ray diffraction study on transition metals in a LHDAC will be a new arsenal in understanding electronic and magnetic transition and the effects of the transition on the physical properties of 3*d* transition metals in oxides and silicates deep within the Earth's interior.

We thank M. Hu, P. Dera, C. Prewitt, C.-S. Yoo, W. Sturhahn, W. A. Bassett, P. Chow and C. C. Kao for their help and discussions. We thank GSECARS, APS for the use of the X-ray facilities and the ruby fluorescence system. VVS acknowledges financial support from the Department of Energy under grant No. DE-FG02-02ER45955. SDJ acknowledges financial support from NSF-EAR-0440112. This work and use of the APS are supported by the US Department

of Energy, Basic Energy Sciences, Office of Science, under contract No. W-31-109-ENG-38, and the State of Illinois under HECA. Work at Carnegie was supported by DOE/BES, DOE/NNSA (CDAC), NSF and the W. M. Keck Foundation.

References

Badro, J., Fiquet, G., Guyot, F., Rueff, J. P., Struzhkin, V. V., Vankó, G. & Monaco, G. (2003). *Science*, **300**, 789–791.

Badro, J., Fiquet, G., Struzhkin, V. V., Somayazulu, M., Mao, H. K., Shen, G. & Bihan, T. Le (2002). *Phys. Rev. Lett.* **89**, 205504.

Badro, J., Rueff, J. P., Vankó, G., Monaco, G., Fiquet, G. & Guyot, F. (2004). *Science*, **305**, 383–386.

Badro, J., Struzhkin, V. V., Shu, J., Hemley, R. J., Mao, H. K., Kao, C. C., Rueff, J. P. & Shen G. (1999). *Phys. Rev. Lett.* **83**, 4101–4104.

Burns, R. G. (1993). *Mineralogical Applications of Crystal Field Theory*. Cambridge University Press.

Cohen, R. E., Mazin, I. I. & Isaak, D. G. (1997). *Science*, **275**, 654–657.

Davis, B. L. & Adams, L. H. (1964). *J. Phys. Chem. Solids*, **25**, 379–388.

Gschneidner, K. A., Elliott, R. O. Jr & McDonald, R. R. (1962). *J. Phys. Chem. Solids*, **23**, 555–566.

Hölzer, G., Fritsch, M., Deutsch, M., Härtwig, J. & Förster, E. (1997). *Phys. Rev. A*, **56**, 4554–4568.

Jacobsen, S. D., Lin, J. F., Shen, G., Prakepenka, V., Dera, P., Angel, R. J., Mao, H. K. & Hemley, R. J. (2005). *J. Synchrotron Rad.* **12**, 577–583.

Jacobsen, S. D., Reichmann, H. J., Spetzler, H., Mackwell, S. J., Smyth, J. R., Angel, R. J. & McCammon, C. A. (2002). *J. Geophys. Res.* **107**, 10.1029/2001JB000490.

Li, J., Struzhkin, V. V., Mao, H. K., Shu, J., Hemley, R. J., Fei, Y., Mysen, B., Dera, P., Prakapenka, V. & Shen, G. (2004). *Proc. Natl. Acad. Sci. USA*, **101**, 14027–14030.

Lin, J. F., Santoro, M., Struzhkin, V. V., Mao, H. K. & Hemley, R. J. (2004). *Rev. Sci. Instrum.* **75**, 3302–3306.

Lin, J. F., Shu, J., Mao, H. K., Hemley, R. J. & Shen, G. (2003). *Rev. Sci. Instrum.* **74**, 4732–4736.

Lin, J. F., Struzhkin, V. V., Jacobsen, S. D., Hu, M., Chow, P., Kung, J., Liu, H., Mao, H. K. & Hemley, R. J. (2005). *Nature (London)*. **436**, 377–380.

Lin, J. F., Struzhkin, V. V., Mao, H. K., Hemley, R. J., Chow, P., Hu, M. & Li, J. (2004). *Phy. Rev. B*, **70**, 212405.

Lin, J. F., Sturhahn, W., Zhao, J., Shen, G., Mao, H. K. Hemley, R. J. (2004). *Geophys. Res. Lett.* **31**, L14611.

Lin, J. F., Sturhahn, W., Zhao, J., Shen, G., Mao, H. K. & Hemley, R. J. (2005). *Advances in High-Pressure Technology for Geophysical Applications*, edited by J. Chen, Y. Wang, T. Duffy, G. Shen & L. Dobrzhinetskaya, pp. 397–411. Elsevier.

Milner, A., Pasternak, M. P., Lee, V. E., Speziale, S. & Jeanloz, R. (2004). *Eos Trans. AGU 85(47)*, Fall Meeting Supplement. Abstract MR14A-05.

Patterson, J. R., Aracne, C. M., Jackson, D. D., Malba, V., Weir, S. T., Baker, P. A. & Vohra, Y. K. (2004). *Phys. Rev. B*, **69**, 220101.

Peng, G., Wang, X., Randall, C. R., Moore, J. A. & Cramer, S. P. (1994). *Appl. Phys. Lett.* **65**, 2527–2529.

Rueff, J. P., Kao, C. C., Struzhkin, V. V., Badro, J., Shu, J., Hemley, R. J. & Mao, H. K. (1999). *Phys. Rev. Lett.* **82**, 3284–3287.

Rueff, J. P., Krisch, M., Cai, Y. Q., Kaprolat, A., Hanfland, M., Lorenzen, M., Masciovecchio, C. & Sette, F. (1999). *Phys. Rev. B*, **60**, 14510–14512.

Rueff, J. P., Krisch, M. & Lorenzen, M. (2002). *High Press. Res.* **22**, 53–56.

Rueff, J. P., Shukla, A., Kaprolat, A., Krisch, M., Lorenzen, M., Sette, F. & Verbena, R. (2001). *Phys. Rev. B*, **63**, 132409.

Santoro, M., Lin, J. F., Mao, H. K. & Hemley, R. J. (2004). *J. Chem. Phys.* **121**, 2780–2787.

Shannon, R. D. & Prewitt, C. T. (1969). *Acta Cryst.* B**25**, 925–946.

Shen, G., Rivers, M. L., Wang, Y. & Sutton, S. R. (2001). *Rev. Sci. Instrum.* **72**, 1273–1282.

Sherman, D. M. (1988). *Structural and Magnetic Phase Transitions in Minerals*, edited by S. Ghose, J. M. D. Coey and E. Salje. New York: Springer-Verlag.

Sherman, D. M. (1991). *J. Geophys. Res.* **96**, 14299–14312.

Sturhahn, W., Jackson, J. M. & Lin, J. F. (2005). *Geophys. Res. Lett.* In the press.

Wang, X., de Groot, F. M. F. & Cramer, S. P. (1997). *Phys. Rev. B*, **56**, 4553–4564.

Yoo, C. S., Maddox, B., Klepeis, J.-H. P., Iota, V., Evans, W., McMahan, A., Hu, M., Chow, P., Somayazulu, M., Häusermann, D., Scalettar, R. T. & Pickett, W. E. (2005). *Phys. Rev. Lett.* **94**, 115502.

Zhao, J., Sturhahn, W., Lin, J. F., Shen, G. & Mao, H. K. (2005). *High Press. Res.* **24**, 447–457.